

## Supplementary Data

**Supplementary Table 1.** The association between plasma IL-6 levels and HCC patient characteristics and median survival months.

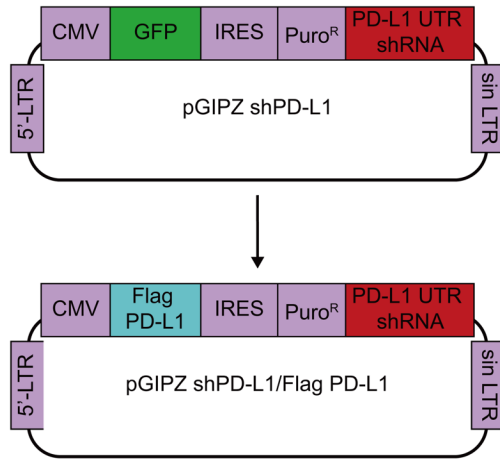
Variable	Low Values N = 60 (%)	High Values N = 43 (%)	P value
<b><u>Sex</u></b>			0.1
Male	39 (65%)	33 (76.7%)	
Females	21 (35%)	10 (23.3%)	
<b><u>Hepatitis (HCV/HBV)</u></b>			0.1
Positive	29 (48.3%)	26 (60.5)	
Negative	31 (51.7)	17 (39.5)	
<b><u>Cirrhosis</u></b>			0.1
Presence	32 (53.3%)	29 (67.4)	
Absence	28 (46.7%)	14 (32.6%)	
<b><u>Child-Pugh</u></b>			0.006
A	8 (13.3%)	4 (9.3%)	
B	48 (80%)	26 (60.5%)	
C	4 (6.7%)	13 (30.2%)	
<b><u>TNM Staging</u></b>			
I_II	25 (49%)	10 (23.8%)	0.03
III-A-III-B	12 (23.5%)	19 (45.2%)	
III-C-IVB	14 (27.5%)	13 (31%)	
<b><u>BCLC Staging</u></b>			0.02
0-B	14 (24.6%)	3 (7%)	
CD	43 (75.4%)	40 (93%)	
<b><u>CLIP Staging</u></b>			0.0001
0-2	37 (72.5%)	14 (33.3%)	
3	10 (19.6%)	13 (31%)	
4-6	4 (7.8%)	15 (35.7%)	
<b><u>Median Survival (95% CI) months</u></b>	19.7 (15-5-23.8)	6.4 (1-16.5)	0.04

**Supplementary Table 2.** Candidates of PD-L1-interacted N-glycosyltransferases were described previously (6) and cataloged via their localization from <http://www.genecards.org/information>. Oligosaccharyl-transferase complex members are labeled as red.

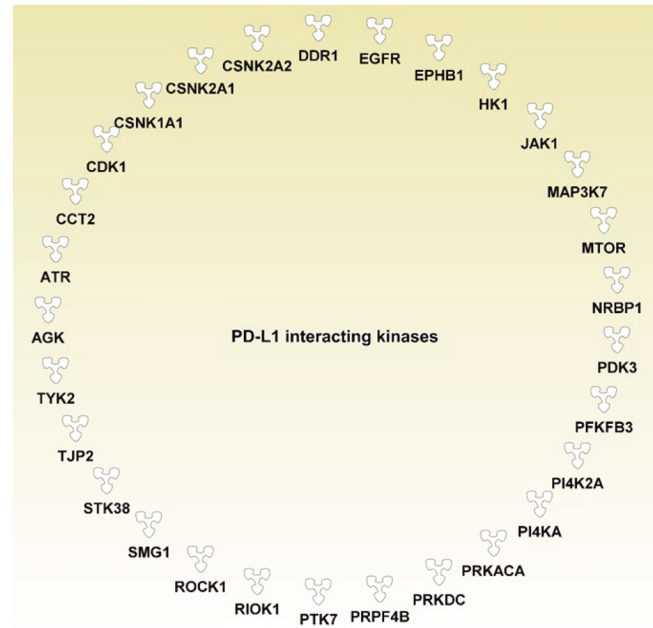
<b>Name</b>	<b>Localization</b>	<b>Other</b>
PGM3	cytosol	
B3GNT3	golgi apparatus	
TMEM165	golgi apparatus	
VCP	nucleus, cytosol and ER	
KRTCAP2	plasma membrane or ER	
MOGS	ER	
ALG8	ER	
DPAGT1	ER	
STT3A	ER	Oligosaccharyl-transferase complex
STT3B	ER	
DDOST	ER	
DAD1	ER	
MGAT4B	ER	
RPN1	ER	
RPN2	ER	

## Supplementary figure 1

A



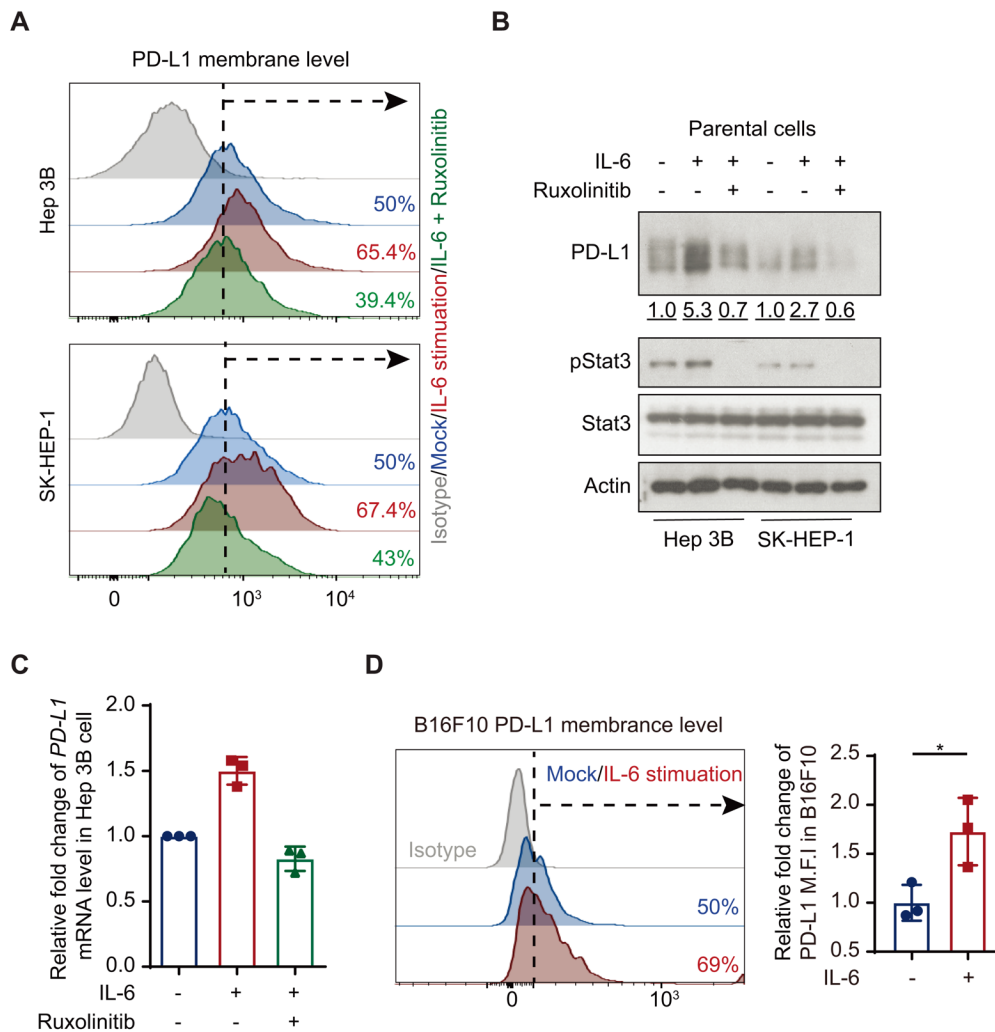
B



### Supplementary Figure 1. Strategy and construction of plasmids for the identification of PD-L1-associated kinases.

(A) Dual expression pGIPZ constructs were used to generate stable cell lines. pGIPZ vectors containing a short hairpin RNA sequence targeting the 3'-untranslated region of human or murine PD-L1 were used as templates. The original green fluorescent protein cDNA was replaced with cDNA from Flag-PD-L1 WT, Y112F, or ngPD-L1 (four glycosylation sites: N35, N192, N200, and N219 to Q). (B) Flag PD-L1 was immunoprecipitated from stable cells using a Flag M2 bead, purified via gel elution after electrophoresis, and subjected to liquid chromatography-tandem mass spectrometric analysis to identify PD-L1 associated partners. The binding proteins were examined using Ingenuity Pathway Analysis to identify Tyr and Ser/Thr kinases.

**Supplementary figure 2**

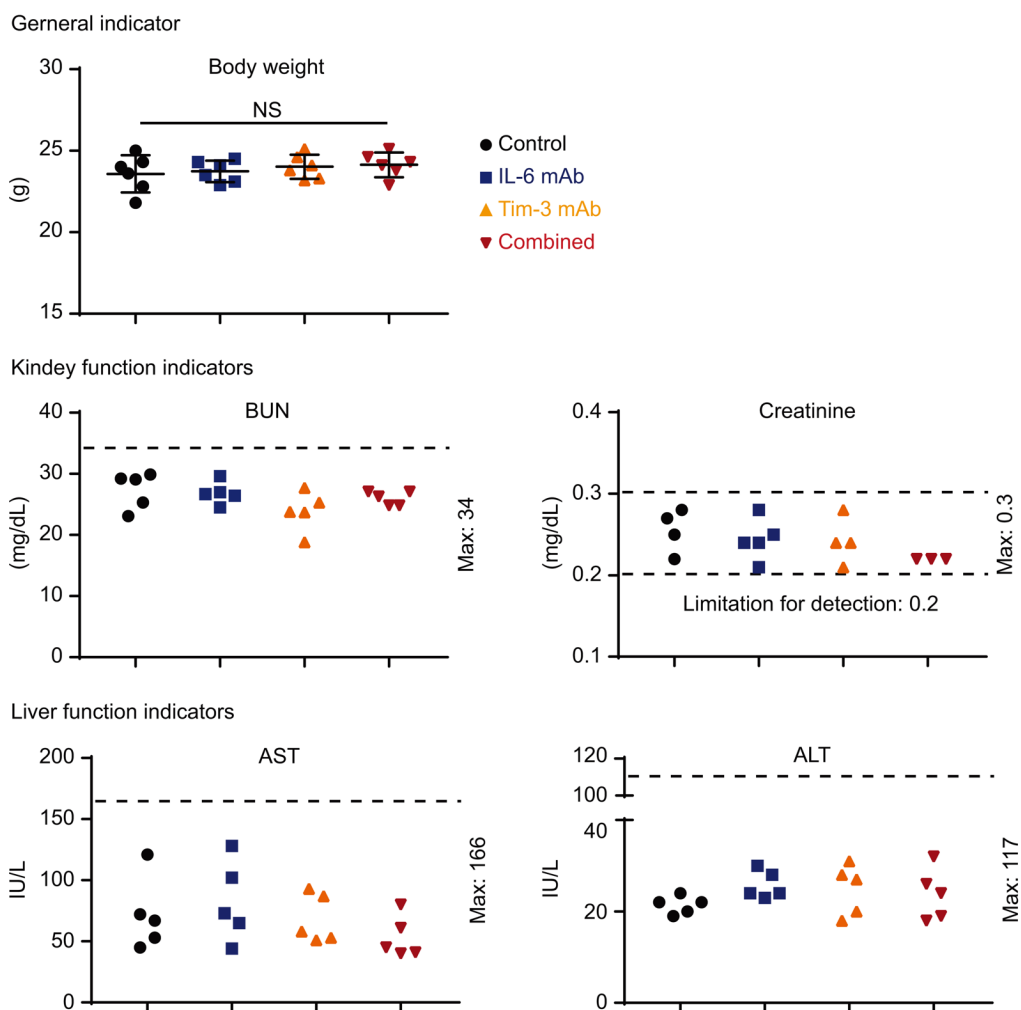


**Supplementary Figure 2. IL-6 upregulates PD-L1 expression in parental HCC cells.**

(A, B, C) Flow cytometric (A), Western blot (B), and quantitative RT-PCR (C) analyses of PD-L1 expression in parental Hep 3B and SK-HEP-1 cells with or without exposure to IL-6 (20 ng/ml) and/or ruxolitinib (10  $\mu$ mol/l) for 18 h. Fold increase in PD-L1 protein expression level after the indicated treatment in Hep 3B or SK-HEP-1 cells (control set to 1) are shown below the blot. Three independent experiments were performed for RT-PCR. Error bars, mean  $\pm$  S.D. (D) Flow cytometric analysis of PD-L1 expression in parental B16F10 cells with or without exposure to mouse IL-6 (25 ng/ml) for 18

h. Data showing relative fold change in the mean fluorescence intensity (M.F.I.) of PD-L1. Error bars represent  $\pm$  S.D. \* $P < 0.05$ , Mann-Whitney test.

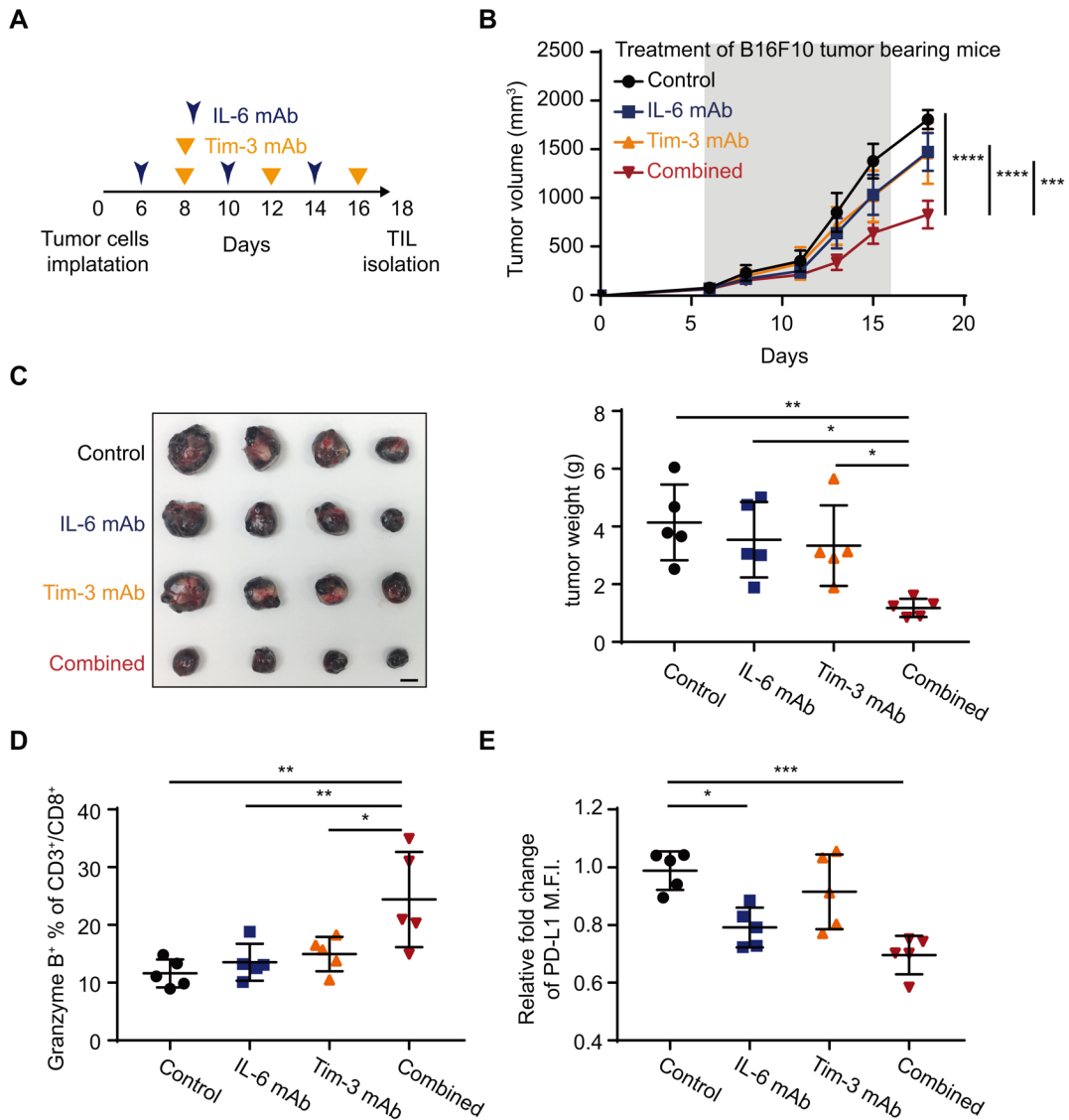
**Supplementary figure 3**



**Supplementary Figure 3. In vivo toxicity detection.**

Body weight, and kidney and liver function indicators in Hepa 1-6 tumor-bearing mice (N = 5) after each indicated treatment. Maximum and normal ranges are indicated by the dashed lines. Error bar, mean  $\pm$  S.D. one-way ANOVA in (A), NS, not significant.

**Supplementary figure 4**

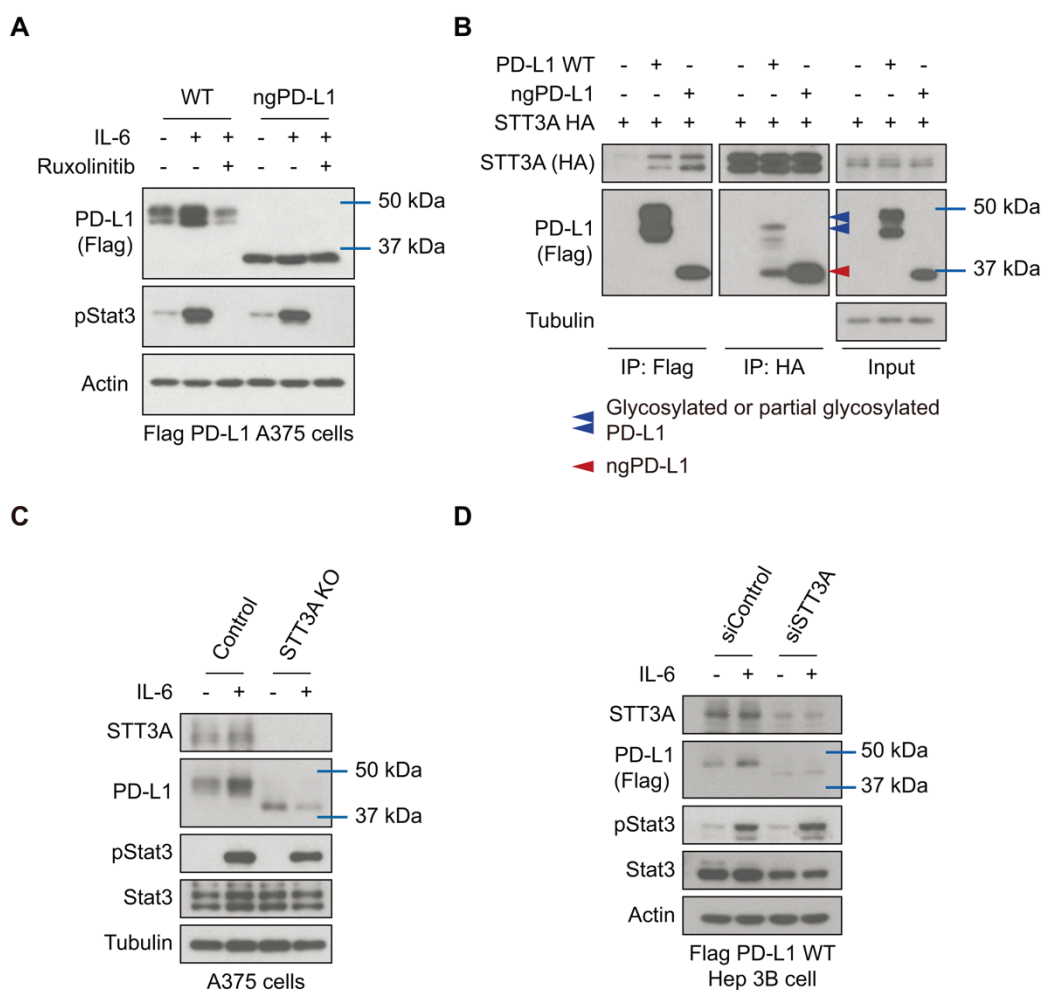


**Supplementary Figure 4. Neutralization of IL-6 in B16F10 tumor-bearing mice enhances the efficacy of anti-Tim-3 mAb therapy.**

(A) Schematic of the treatment schedule for the combination of IL-6 and Tim-3 mAbs in B16F10 tumor bearing mice. (B) Tumor growth in mice bearing B16F10 tumors were administered IL-6 mAb, Tim-3 mAb, or the combination (N = 8). The gray box in each panel indicates the duration of treatment. (C) Tumor size and weight (N = 5) of mice administered the indicated treatment. Scale bar, 1 cm. (D) Flow cytometric analysis of granzyme B-positive CD3<sup>+</sup>/CD8<sup>+</sup> T cells in B16F10 tumors subjected to

the indicated treatments (N = 5). (E) Flow cytometric analysis of the cell surface expression of PD-L1 from B16F10 tumors subjected to the indicated treatment ( $n = 5$ ). Error bars, mean  $\pm$  S.D. \* $P < 0.05$ , \*\* $P < 0.01$ , \*\*\* $P < 0.001$ , and \*\*\*\* $P < 0.0001$ , repeated-measures ANOVA in (B), and one-way ANOVA in (C), (D) and (E).

**Supplementary figure 5**



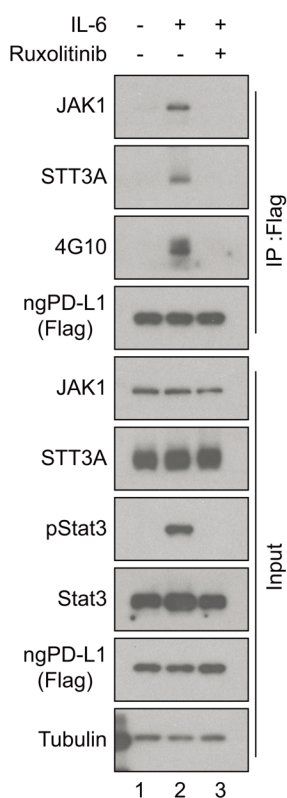
**Supplementary Figure 5. The IL-6/JAK1 pathway upregulates PD-L1 WT through glycosylation process and was blocked by STT3A knockout in melanoma cells.**

(A) Western blot (WB) analysis of exogenous PD-L1 expression in WT and ngPD-L1 A375 cells with or without exposure to IL-6 (20 ng/ml) and/or ruxolitinib (10  $\mu$ mol/L) for 18 h. (B) Immunoprecipitation (IP) followed by WB analysis of STT3A or PD-L1 level in Hep3B cells transfected with the indicated plasmid. (C) Western blot analysis of the indicated proteins in control and STT3A knockout A375 cells with or without exposure to IL-6 (20 ng/ml) for 18 h. (D) WB analysis

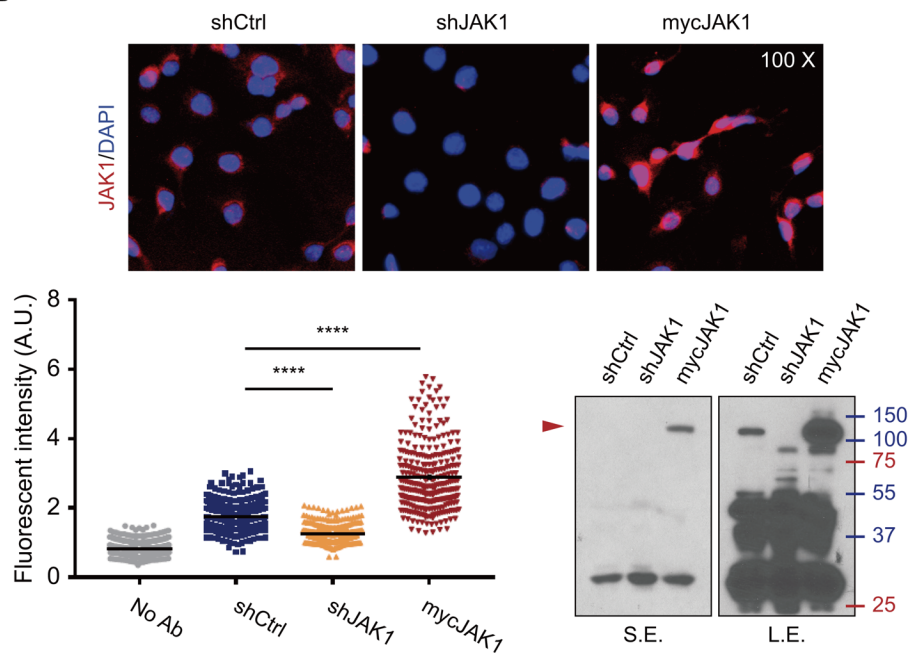
of the indicated proteins in control and STT3A knockdown Flag-PD-L1 WT-Hep3B cells with or without exposure to IL-6 (20 ng/ml) for 18 h.

**Supplementary figure 6**

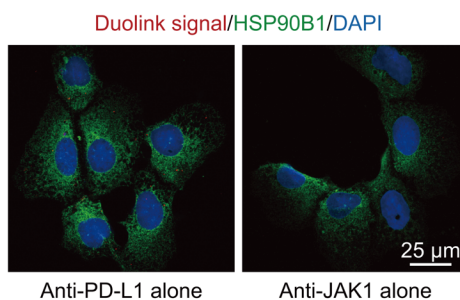
**A**



**B**



**C**

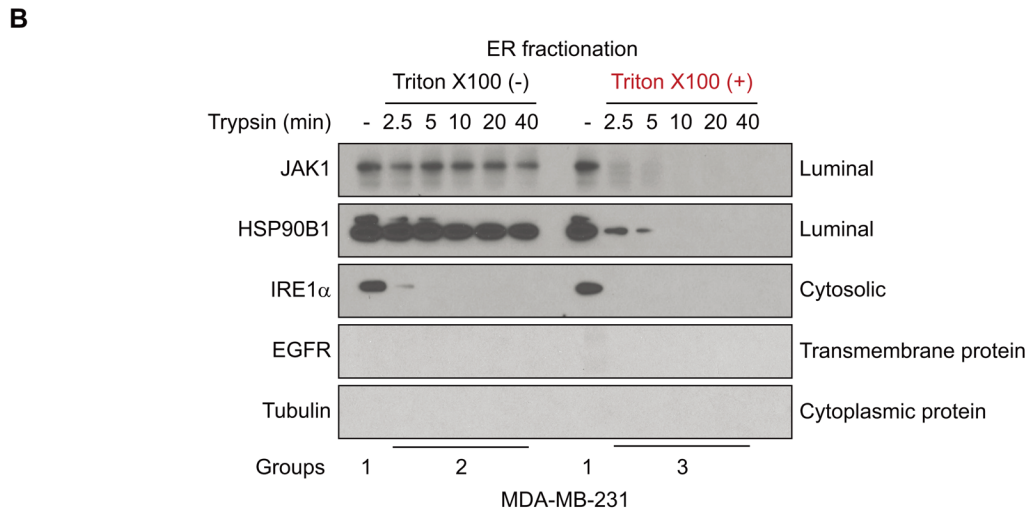
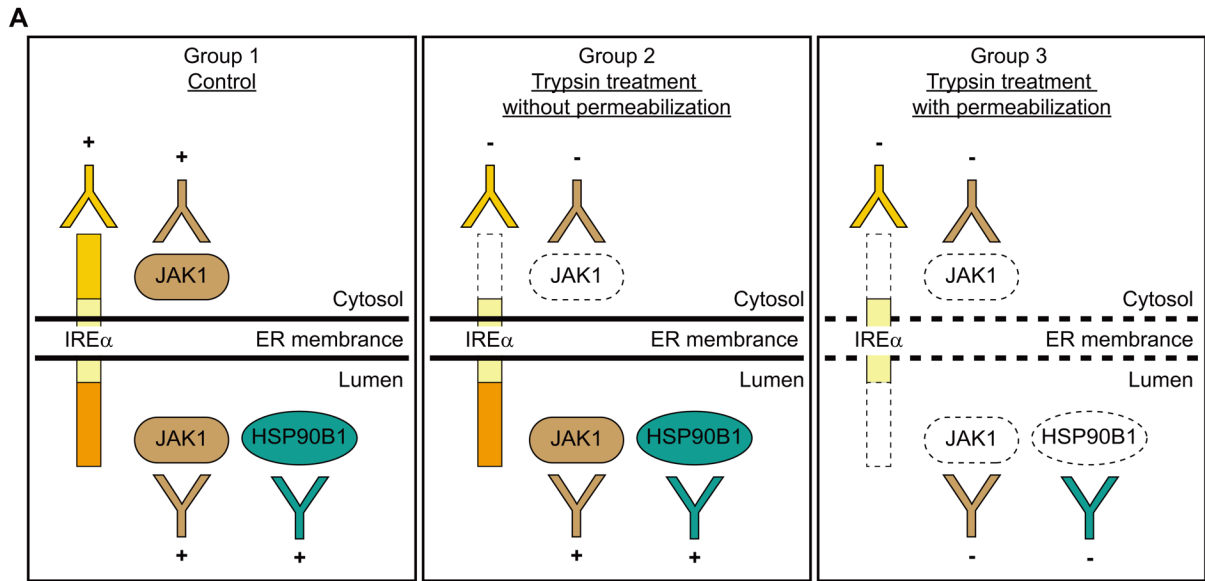


**Supplementary Figure 6. The IL-6 enhances PD-L1 tyrosine phosphorylation and STT3A association**

(A) IP followed by WB analysis of JAK1, STT3A, and ngPD-L1 tyrosine phosphorylation (4G10) in Flag-ngPD-L1-Hep 3B cells with or without exposure to IL-6 (20 ng/ml) and ruxolitinib (10 μmol/L) for 30 min. (B) Characterization of the JAK1 antibody for immunofluorescence staining. Hep 3B

control short hairpin RNA (shCtrl), JAK1 knockdown short hairpin RNA (shJAK1), and JAK1 overexpressing (mycJAK1) cells were subjected to immunofluorescence staining and WB analysis with JAK1 antibody (Cat. No. sc-376996). Representative images of JAK1 staining in different cells. Magnification, 100×. Quantitation of immunofluorescence staining are described in Materials and Methods. S.E., short exposure; L.E., long exposure. Error bars, means  $\pm$  SD. \*\*\*\* $P < 0.0001$ , one-way ANOVA. (C) Negative control for Duolink assay of JAK1 and PD-L1 interaction in Hep 3B cells. The red dots indicate their interaction. Green fluorescence (HSP90B1) was used as endoplasmic reticulum (ER) marker, and DAPI as a nuclear marker. Scale bar, 25  $\mu$ m.

**Supplementary figure 7**

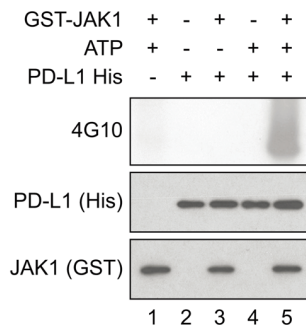


**Supplementary Figure 7. Model illustrating trypsinization of the ER fractions.**

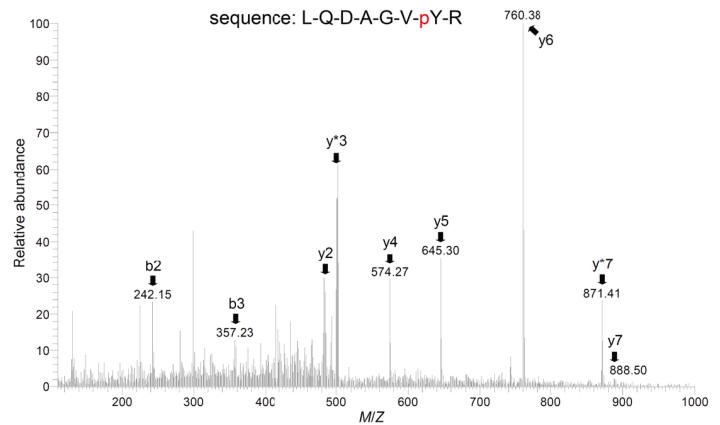
(A) ER fraction without trypsin. All markers can be detected (group 1). ER fraction subjected to trypsin digestion without permeabilization. Cytosolic portions of ER proteins were not detected after digestion whereas luminal portions of ER proteins were detected (group 2). ER fraction subjected to trypsin digestion with permeabilization (1% Triton X-100). No markers were detected (group 3). (B) Trypsin digestion of ER fractions without (group 2) or with permeabilization (group 3) in MB-231 cells.

## Supplementary figure 8

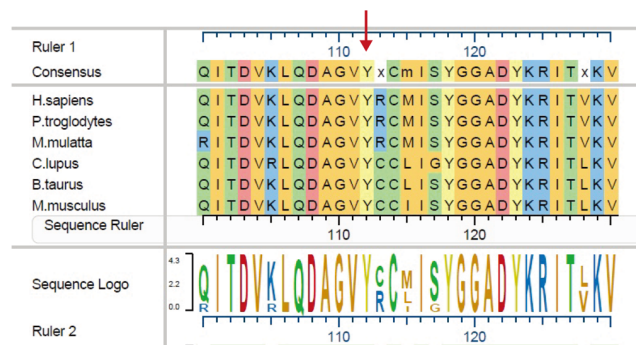
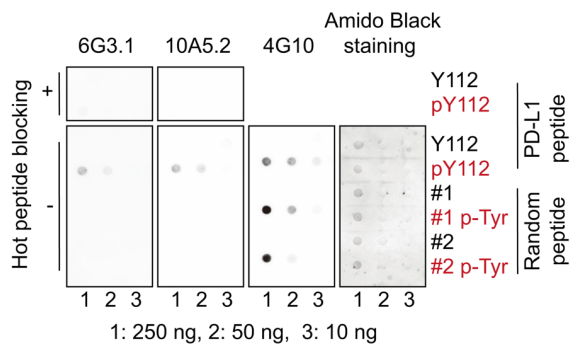
**A**



**B**



**C**

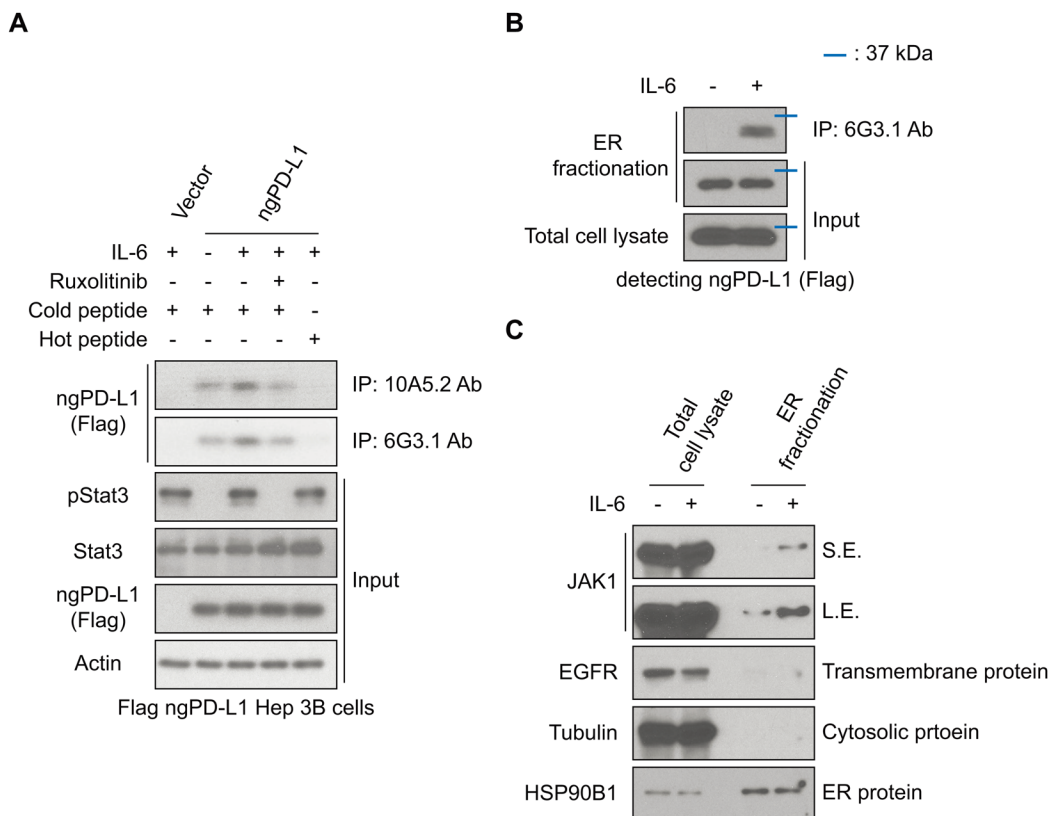


### Supplementary Figure 8. JAK1 phosphorylates ngPD-L1 at Y112.

(A) Recombinant ngPD-L1 protein from the pET 21a system was subjected to an in vitro kinase assay under the indicated conditions followed by Western blot (WB) analysis to detect Tyr phosphorylation using 4G10 antibody. (B) Tyrosine 112 phosphorylation of PD-L1 was detected by liquid chromatography-tandem mass spectrometric analysis. Sequence alignment of Y112 PD-L1 across different species. (C) Characterization of the PD-L1 pY112 antibodies generated by dot blotting. The antibody specifically recognizes the hot peptide (pY112) but not the cold peptide (Y112) or the other random peptides with Tyr phosphorylation (p-Tyr). This specific reaction of the PD-L1 pY112 antibody was completely neutralized by excessive amount of the PD-L1 pY112 hot peptide. 4G10

antibody was used to detect p-Tyr on pY112 PD-L1 peptide, random #1 and #2 peptide. Amido black staining was performed to show peptides on the nitrocellulose membrane.

**Supplementary figure 9**



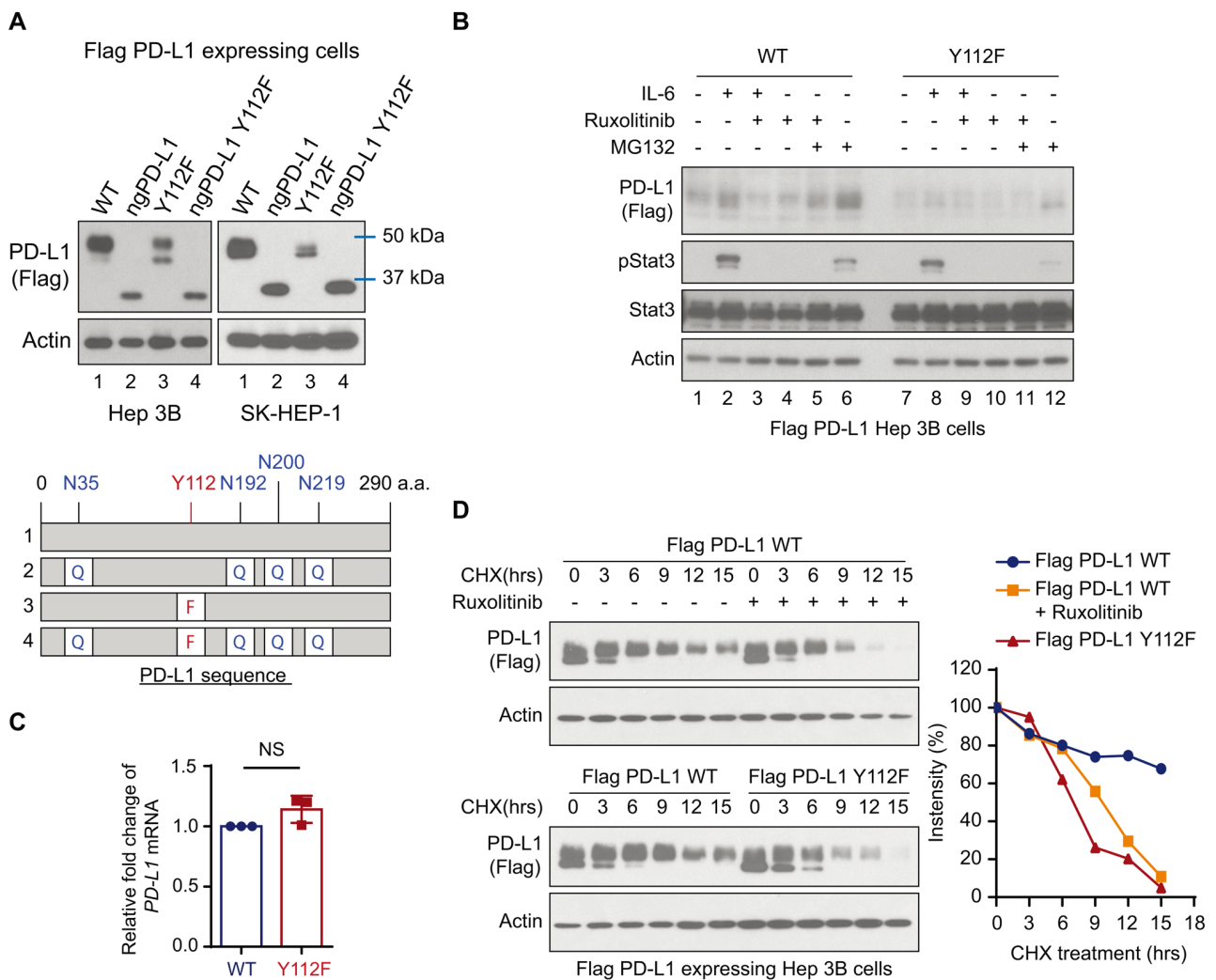
**Supplementary Figure 9. IL-6 induces JAK1 translocation and phosphorylates ngPD-L1 at Y112**

**in ER region**

(A) Results of IP followed by WB analysis to determine ngPD-L1 pulled down levels in Flag-ngPD-L1-Hep 3B cells treated with or without IL-6 (20 ng/ml, 30 min) and/or ruxolitinib (10 μmol/L, 30 min) using the indicated antibodies, which were preincubated with cold or hot peptides (pY112F PD-L1 peptide). (B) Results of IP followed by WB analysis to determine ngPD-L1 pulled down levels in

ER fractions from Flag-ngPD-L1-Hep 3B cells treated with or without IL-6 (20 ng/ml, 30 min) using the 6G3.1 antibody. (C) WB analysis of total cell lysates or ER fractions from Flag-ngPD-L1-Hep 3B cells with or without IL-6 stimulation (20 ng/ml, 30 min).

### Supplementary figure 10



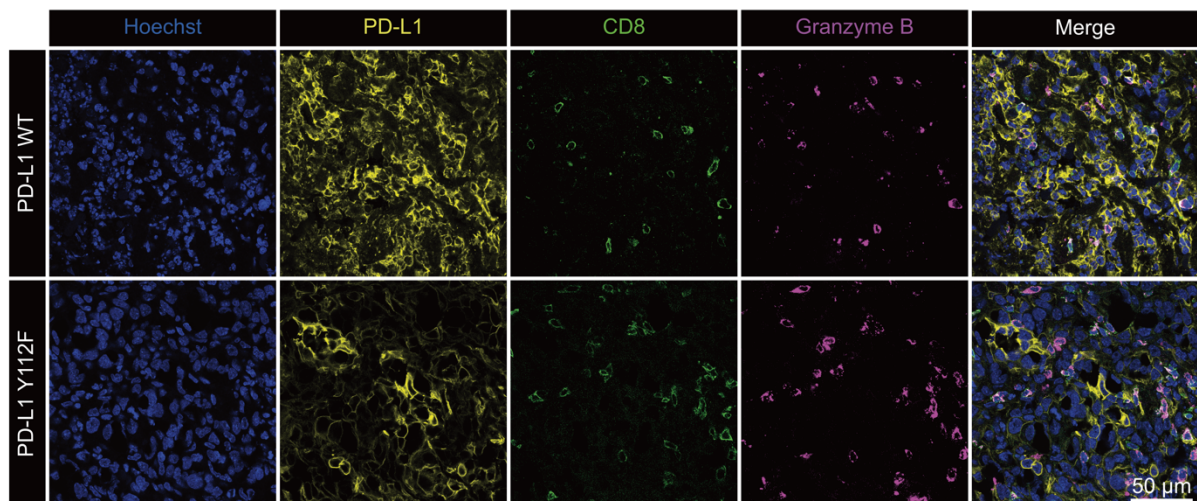
### Supplementary Figure 10. Y112F mutation reduces PD-L1 protein half-life.

(A) Top, Western blot (WB) analysis of lysates from exogenous PD-L1 expressing Hep 3B and SK-HEP-1 cells. Bottom, Schematic diagram of various PD-L1 mutants used in this study. The numbers

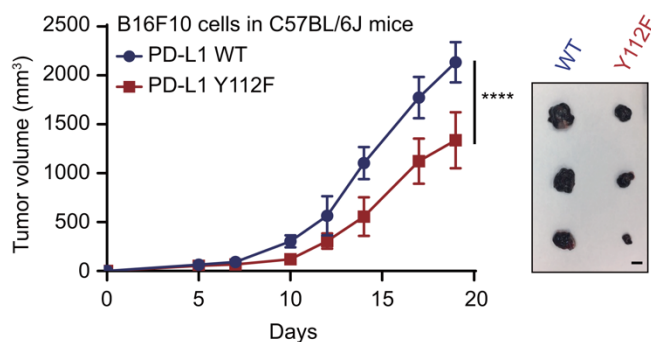
indicate the amino acid position of PD-L1. (B) WB analysis of exogenous PD-L1 expression in Flag-PD-L1 WT-Hep 3B or Y112F-Hep 3B cells with or without exposure to IL-6 (20 ng/ml, 18 h), ruxolitinib (10  $\mu$ mol/L, 18 h), and/or MG132 (10  $\mu$ mol/L, 6 h). (C) Quantitative RT-PCR analysis of RNA from PD-L1 WT and PD-L1 Y112F Hep 3B cells. Experiments were repeated independently three times. Error bars, mean  $\pm$  S.D. NS, not significant, Mann-Whitney test. (D) WB analysis of Flag PD-L1 WT- or Y112F-Hep 3B cells treated with cycloheximide (CHX; 50  $\mu$ M) or ruxolitinib (10  $\mu$ M) for the indicated times.

### Supplementary figure 11

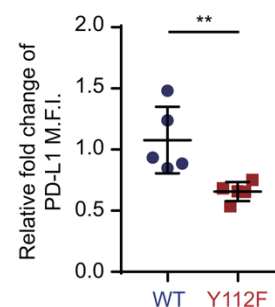
**A**



**B**



**C**



**Supplementary Figure 11. Tumor progression of PD-L1 WT and Y112F cells in Hepa 1-6 or B16F10 tumor bearing immunocompetent mice.**

(A) Representative immunofluorescence staining of PD-L1, CD8, and granzyme B expression in the indicated Hepa 1-6 stable cell-generated tumors. Scale bar, 50  $\mu$ m. (B) Tumor growth and size of PD-L1 WT-B16F10 or Y112F-B16F10 tumors in immunocompetent mice (N = 6). Scale bar, 1 cm. (C) Flow cytometric analysis of cell surface PD-L1 from PD-L1 WT- B16F10 and Y112F- B16F10 tumors ( $n = 5$ ). The relative fold change of the mean fluorescence intensity (M.F.I.) of PD-L1 is shown. Error bars, mean  $\pm$  S.D.  $**P < 0.01$  and  $****P < 0.0001$ , repeated-measures ANOVA in (B) and Mann-Whitney test in (C). NS, not significant.